

FAST IMPLEMENTATION OF ITERATIVE ADAPTIVE APPROACH FOR WIDEBAND UNAMBIGUOUS RADAR DETECTION

Nikita PETROV, Francois LE CHEVALIER

Delft University of Technology, Delft, the Netherlands
 E-mails: N.Petrov@tudelft.nl, F.LeChevalier@tudelft.nl

ABSTRACT

Wideband radars are sensors of new generation used for target detection and classification. Detection of moving targets with wideband radar faces range migration phenomenon which is used to resolve velocity ambiguities in low pulse repetition frequency mode. The resolution is equivalent to a bi-dimensional spectrum estimation problem with non-uniform sampling, while the ability to resolve velocity ambiguity depends on spectral resolution of the method used. Recently Iterative Adaptive Approach (IAA) was shown an attractive solution of this problem. Nevertheless straightforward implementation of IAA for wideband signal suffers from high computational requirements. In this paper fast implementation of IAA for wideband data is proposed and studied with numerical simulations. Proposed solution decreases computational cost by an order of magnitude for realistic data sizes.

Index Terms—Iterative Adaptive Approach (IAA), wideband radar, target detection, target migration

1. INTRODUCTION

Radar detection of moving targets in presence of clutter is usually performed by pulse-Doppler processing. However, this technique has some limitations coming from the relation between the ambiguous velocity V_a and the ambiguous range R_a [1].

Recently wideband (WB) radars have attracted significant attention due to their advantages for target detection and classification obtained from high range resolution (HRR). However, detection of moving targets with WB radar faces new phenomena coming from the fact that fast moving targets are likely to migrate from one resolution cell to another during the coherent processing interval (CPI) [1]. This phenomena leads to a peak loss in Doppler processing output, and must be compensated in many applications e.g. [2]. On the other hand, if low PRF mode is used, it becomes possible to take advantage of this range walk to mitigate velocity ambiguities.

Several references have considered taking into account range migration in target signature. Compared to the usual narrowband model, it consists in adding a cross-coupling term in the fast-frequency/slow-time domain [1, 3]. Cor-

rect estimation of this term together with Doppler and range components provides ability to detect moving targets unambiguously. According to WB target model discussed previously [1, 3] and revised in the next section, the objective is a bi-dimensional spectrum estimation problem with defined non-uniform sampling case [3].

Recently nonparametric Iterative Adaptive Approach (IAA) was proposed in [4] providing super resolution without strong restrictions on sampling scheme. In addition, this approach does not require sparsity implicitly and so it can deal more easily than most compressive sensing approaches with clutter. These facts make IAA a good choice for wideband unambiguous target detection.

On the other hand, modern radars tends not only to increase the bandwidth and improve range resolution, but also to shift the band to higher frequencies. The difference of migrations at adjacent ambiguities (used to resolve them) depends on the relative bandwidth and the number of pulses in CPI:

$$\rho = \frac{V_a M T_r}{\delta_R} = M \frac{B}{f_0}, \quad (1)$$

where ρ – migration in resolution cells, M – pulses in CPI, T_r – pulse repetition interval (PRI), B – bandwidth, f_0 – carrier frequency (it is assumed that signal occupies frequency band $[f_0: f_0 + B]$), $\delta_R = c/(2B)$ – radar range resolution, $V_a = \lambda_0/(2T_r)$ – ambiguous velocity, λ_0 – carrier wavelength. Hence, radars with the same range resolution working at higher frequencies require more pulses to be processed in order to obtain the same migration at ambiguity velocity. This leads to significant increase of data size and enormous growth of IAA computational complexity.

Several algorithms for fast implementation of IAA were recently found [5, 6], but all of them are strongly limited to uniform sampling, thus they cannot be applied for the problem under consideration. On the other hand, wideband Coherent Integration (CI) used for target focusing in range-velocity domain can be implemented in a very efficient way with two fast Fourier transforms (FFT) and Keystone transform [7]. This processing is used in this paper to decrease the computational cost of existing implementation of IAA.

Notations: we denote vectors and matrices with boldface lowercase and boldface uppercase respectively. Notation $\mathbf{A}_{l,i}$ is used for matrix element at l -th line and i -th column; $\mathbf{A}_{*,i}$ and $\mathbf{A}_{l,*}$ are used for i -th column and l -th line

The work is funded by Dutch Technology Foundation (STW)

of the matrix respectively. Curly brackets $y\{x\}$ are used to denote function y of argument x .

This paper is organized as follows. In section 2, the model of a moving target in WB radar is presented. In sections 3 and 4, IAA and fast CI algorithms are revisited. Fast implementation of IAA is carefully explained in section 5. An expected improvement is shown via numerical simulations in section 6. Finally, conclusions are drawn in section 7.

2. DATA MODEL

Herein a pulse-Doppler radar with wideband waveform is considered. A range migration of a moving scatterer at blind velocity is assumed to be negligible within one PRI, but significant during the whole CPI: $V_a T_r \ll \delta_R$ and $V_a M T_r > \delta_R$, where V is the (constant) radial velocity of the scatterer. A low PRF is considered so that no range ambiguities occur but the maximal Doppler frequency is aliased around ambiguous velocity V_a , and the maximum velocity expected for a target $V_{max} > V_a$.

In case of a wideband waveform, a moving target migrates so the detection should be performed after range compression on a block of K adjacent range cells called low range resolution (LRR) segment [3]. The samples to be processed can thus be represented by a $K \times M$ matrix where the first and second dimensions refer, respectively, to the fast- and slow-time. However, the data model can be more conveniently expressed after FFT on the fast-time - in the fast-frequency/slow-time domain. Taking into account HRR of the radar, both clutter and targets can be modelled as multiple scatterers. Then $K \times M$ data matrix can finally be expressed as:

$$\mathbf{Y} = \sum_{d=1}^D x_d \mathbf{Z}(d) + \mathbf{N}, \quad (2)$$

where D , x_d , represent, respectively, the number of scatterers and the d -th complex amplitude, $\mathbf{Z}(d)$ is a $K \times M$ matrix containing target signature and \mathbf{N} is the receiver noise. The receiver noise is assumed to be a bi-dimensional spectrally white Gaussian random process with power σ^2 .

The scatterer signature \mathbf{Z} involved in (2) was studied earlier in e.g. [1, 3] and was shown to be the product of a two-dimensional (2D) cisoid with cross-coupling term. More precisely, the (k, m) -th element (where $m = 0 \dots M-1$, $k = 0 \dots K-1$) of the matrix \mathbf{Z} can be expressed by:

$$\mathbf{Z}_{k,m}(t, v) = \exp(2\pi j(f_r(t)k + f_D(v)m(1 + \mu k))) \quad (3)$$

where $f_r(t), f_D(v)$ – range and Doppler frequencies of a hypothesis (t, v) and $\mu = B/(f_0 K)$. Assume that hypotheses are limited by LRR in range and by velocities of interest such as: $t = 0 \dots N_t - 1$, $v = 0 \dots N_v - 1$. Then

$$f_r(t) = -\frac{t}{N_t} = -\frac{t}{\gamma_t K} \quad (4)$$

is the range (fast-time) frequency corresponding to the target with time delay $\tau = t/B$, and γ_t is an oversampling (zero padding) factor in range. Range frequencies f_r have

values in the interval $[-1, 0]$. In much the same way the Doppler frequency is defined:

$$f_D(v) = \frac{v - N_v/2}{N_v/N_a} = \frac{v - N_v/2}{M\gamma_v}, \quad (5)$$

where γ_v – oversampling factor in velocity, N_a – integer number of velocity ambiguities of interest and $N_v = M\gamma_v N_a$ is a total number of velocity hypothesis. Target velocity at hypothesis v can be expressed by: $V = v\delta_v = vV_a/(M\gamma_v)$. Assuming that the velocities of interest are symmetric around zero, velocity (Doppler) frequency f_D becomes spread over the interval $[-N_a/2, N_a/2]$.

The same equation can be rewritten:

$$\mathbf{Z}_{k,m}(t, v) = \exp(2\pi j(f_r(t)k + f_D(v)m')), \quad (6)$$

where $m' = m(1 + \mu k)$. Hence it can be interpreted as a bi-dimensional cisoid sampled at a rate depending on the subband. Such a sampling scheme is obviously different from the bi-dimensional uniform sampling; hence it provides an ability to unfold velocity ambiguity.

A vectorization of all range-velocity steering vectors is applied to come to a standard expression of the received signals (10). In case of a target at range cell t and velocity cell v , its signature is a vector \mathbf{z} of length $L=KM$. Index $l=0 \dots L-1$ combines line slow-time index $m = [l/K]$ and fast-frequency index $k = l - [l/K]K$, where $[\cdot]$ is rounding towards lower integer operator:

$$\mathbf{z}_l(t, v) = \exp \left\{ 2\pi j \left(f_r(t) \left(l - K \left[\frac{l}{K} \right] \right) \right. \right. \\ \left. \left. + f_D(v) \left[\frac{l}{K} \right] \left(1 + \mu \left(l - K \left[\frac{l}{K} \right] \right) \right) \right) \right\} \quad (7)$$

Range and velocity hypothesis are also vectorised in a row with index $i = t + N_t v$, $i = 0 \dots N_t N_v - 1$. Matrix \mathbf{A} of the steering vectors is defined by substitution index i instead of t and v in vectorised target signature:

$$\mathbf{A}_{l,i} = \exp \left(2\pi j \left(f_r \left(i - N_t \left[\frac{i}{N_t} \right] \right) \left(l - K \left[\frac{l}{K} \right] \right) \right. \right. \\ \left. \left. + f_D \left(\left[\frac{i}{N_t} \right] \right) \left[\frac{l}{K} \right] \left(1 + \mu \left(l - K \left[\frac{l}{K} \right] \right) \right) \right) \right). \quad (8)$$

The target signatures being given by (3), the received signal can be obtained by:

$$\mathbf{Y} = \sum_{t=1}^{N_t} \sum_{v=1}^{N_v} \mathbf{X}_{t,v} \mathbf{Z}(t, v) + \mathbf{N}, \quad (9)$$

where matrix \mathbf{X} of size $N_t \times N_v$ contains complex amplitudes of the range-velocity map of interest. An equivalent vector notation exploiting previously discussed matrix \mathbf{A} can be used:

$$\mathbf{y} = \mathbf{Ax} + \mathbf{n}, \quad (10)$$

where $\mathbf{y} = \text{vec}(\mathbf{Y})$ and $\mathbf{x} = \text{vec}(\mathbf{X})$ are vectorised counterparts of corresponding matrices.

Fourier-based technique taking into account target migration and called wideband CI thus can be done in a matrix notation by:

$$\mathbf{x} = \mathbf{A}^H \mathbf{y} / (KM), \quad (11)$$

where $(\cdot)^H$ stands for Hermitian transpose. Computational complexity of this operation is $O(N_t N_v KM)$.

3. ITERATIVE ADAPTIVE APPROACH FOR WIDEBAND DATA

In this section IAA described in [4] is revisited for the vectorised signal model from the previous section. Herein the single snapshot case of IAA is discussed. IAA is divided into three main steps at each iteration. Computational complexity of each step is estimated separately per one iteration.

3.1. Calculate covariance matrix \mathbf{R}

Let \mathbf{P} be $N_t N_v \times N_t N_v$ diagonal matrix whose diagonal contains the power of scatterer at every possible range and velocity cell obtained from the previous iteration of the algorithm (or the output of CI in case of the first iteration). Then i -th diagonal element of \mathbf{P} is:

$$P_{i,i} = |\mathbf{x}_i|^2. \quad (12)$$

IAA covariance matrix is obtained by:

$$\mathbf{R} = \mathbf{A} \mathbf{P} \mathbf{A}^H. \quad (13)$$

For the problem under consideration \mathbf{A} is not a Vandermonde matrix, hence matrix \mathbf{R} is not Toeplitz and cannot be computed by FFT as it is done in [5]. Multiplication $\mathbf{A} \mathbf{P}$ is very fast due to sparsity of matrix \mathbf{P} , on the other hand the second matrix multiplication has high complexity of $O((KM)^2 N_t N_v)$ operations.

3.2. Inverse of covariance matrix \mathbf{R}

Inverse of covariance matrix \mathbf{R} requires $O((KM)^3)$ operations. Due to the fact that oversampling is needed to obtain high resolution $KM < N_t N_v$ so this step is typically tens times faster than step 1.

3.3. Update complex amplitudes

This step is done by:

$$\mathbf{x}_i = \frac{\mathbf{a}^H(i) \mathbf{R}^{-1} \mathbf{y}}{\mathbf{a}^H(i) \mathbf{R}^{-1} \mathbf{a}(i)}, \quad (14)$$

where $\mathbf{a}(i)$ is the steering vector of i -th range-velocity hypothesis (i -th column of matrix \mathbf{A}), so it requires $O((KM)^2 N_t N_v)$ operations.

To sum it up, IAA implementation requires $O((KM)^2 N_t N_v)$ operations limiting its application only to small data sets.

4. FAST COHERENT INTEGRATION

Fast coherent integration is implemented according to [7] in 4 steps and uses signals in non-vectorised form:

1) Oversample signal \mathbf{Y} in slow time by the number of velocity ambiguities of interest N_a to obtain \mathbf{Y}^{up} ;

2) Apply FFT on slow-time to obtain signal in fast-frequency / velocity domain:

$$\mathbf{W}_{f,v'} = \sum_{m=0}^{M-1} \mathbf{Y}_{f,m}^{up} \exp(-2\pi m f_{v'}); \quad (15)$$

3) Inverse Keystone transform is applied to $\mathbf{W}_{f,v'}$ in order to compensate for range migration:

$$\mathbf{W}_{f,v} = \mathbf{W}_{f,v'}|_{v=v'(1+\mu k)}; \quad (16)$$

4) IFFT on fast-frequency is calculated at the last step to obtain range-velocity map (here IFFT has a sign of FFT due to negative values of f_t):

$$\mathbf{X}_{t,v} = \frac{1}{K} \sum_{k=0}^{K-1} \mathbf{W}_{f,v} \exp(-2\pi k f_t). \quad (17)$$

Note that after Keystone transform the signal at higher frequencies of the band (subband $K-1$) is defined for velocities up to $N_a V_a / (2(1 + \mu K)) = N_a V_a / (2(1 + B/f_0))$, while the velocities of interest are limited by $N_a V_a / 2$. We suggest to increase the oversampling factor until all hypothesis of interest are covered (typically increase N_a by 1 is enough) and keep the output samples corresponding to the velocities of interest. An extra normalization by the term $1/M$ is required to obtain the correct amplitude.

Zero-padding should be applied to achieve good quality of interpolation (typically by a factor of 4 [7]). It is also required by IAA to achieve high resolution. The quality of fast CI depends on the interpolation method used at step 2. According to results in [7] spline interpolation provides lower error, while linear interpolation is more attractive from computational aspect.

Apart from presented transform, implementation of IAA requires an inverse operation. It is clear that it can be done in a similar fast implementation with a reverse order of steps and corresponding substitution FFT for IFFT (and the other way round) and applying Keystone transform instead of its inverse version on step 3. The final step is a downsampling operation in this case.

In the next section fast CI is denoted by $\mathbf{X} = \Theta\{\mathbf{Y}\}$ and its inverse analogue by $\mathbf{Y} = \Theta^{-1}\{\mathbf{X}\}$. Moreover, the transforms discussed in this section are applied to matrices, while IAA is implemented using their vectorised counterparts. Fast CI and its inverse analogue are applied to vectors denoted by $\mathbf{x} = \Theta\{\mathbf{y}\}$ and $\mathbf{y} = \Theta^{-1}\{\mathbf{x}\}$ and implemented by additional reconstruction of the matrices from corresponding vectors and vectorization of the outputs.

Computational complexity of the fast implementation of CI is: $O(KN_v \log_2(N_v N_t)) + KO_I$, where O_I is computational complexity of interpolation at step 3. In case of linear interpolation $O_I = O(N_v)$, while spline interpolation requires $O_I = O(N_v + \log_2(N_v))$. Asymptotically computational burden comes from FFTs, thus interpolation term can be ignored.

5. FAST IMPLEMENTATION OF ITERATIVE ADAPTIVE APPROACH FOR WIDEBAND DATA

In this section fast implementation of IAA for wideband unambiguous detection is discussed. The proposed solution is carefully explained with respect to each step of IAA presented in section 3.

5.1. Calculate covariance matrix \mathbf{R}

One of the most computationally expensive steps is estimating of matrix \mathbf{R} by (13).

We propose to first compute $\mathbf{Q} = \mathbf{P}\mathbf{A}^H$, where \mathbf{Q} is $N_vN_t \times KM$ matrix. Then matrix \mathbf{R} can be computed column-wise via fast CI from \mathbf{Q} by:

$$\mathbf{R}_{*,i} = \Theta^{-1}\{\mathbf{Q}_{*,i}\}. \quad (18)$$

Matrix \mathbf{Q} can also be obtained column-wise by $\mathbf{Q}_{*,i} = \mathbf{p} \odot (\mathbf{A}_{i,*})^H$, where $\mathbf{p} = \text{diag}(\mathbf{P})$ is N_vN_t -length column vector and \odot stands for Hadamard product. Thus

$$\mathbf{R}_{*,i} = \Theta^{-1}\{\mathbf{p} \odot (\mathbf{A}_{i,*})^H\}. \quad (19)$$

Covariance matrix \mathbf{R} can be estimated through KM fast CI. Computational complexity of this step is $O(K^2MN_v \log_2(N_vN_t))$.

5.2. Inverse of covariance matrix \mathbf{R}

Matrix \mathbf{R} is non-Toeplitz anymore because of non-uniform sampling scheme. Nevertheless, it is still Hermitian and thus it can be inverted in $(KM)^3/2$ operations [8].

5.3. Update complex amplitudes

Amplitude estimation of IAA can be divided into estimation of numerator and decimator of:

$$\mathbf{x}_i = \frac{\mathbf{a}^H(i)\mathbf{R}^{-1}\mathbf{y}}{\mathbf{a}^H(i)\mathbf{R}^{-1}\mathbf{a}(i)} = \frac{\mathbf{n}_i}{\mathbf{d}_i}. \quad (20)$$

The vector \mathbf{n} can be efficiently estimated in two steps. First, column vector $\boldsymbol{\phi}$ of length KM is obtained by multiplication $\mathbf{R}^{-1}\mathbf{y}$ in $(KM)^2$ operations. The second step is just fast CI applied to $\boldsymbol{\phi}$:

$$\mathbf{n} = \Theta\{\boldsymbol{\phi}\} = \Theta\{\mathbf{R}^{-1}\mathbf{y}\}, \quad (21)$$

which requires $O(KN_v \log_2(N_vN_t))$ operations.

The denominator is a diagonal of the matrix $\boldsymbol{\Psi}$:

$$\boldsymbol{\Psi} = \mathbf{A}^H\mathbf{R}^{-1}\mathbf{A} = \mathbf{G}\mathbf{A}, \quad (22)$$

where matrix \mathbf{G} of size $N_vN_t \times KM$ can be efficiently computed column-wise via KM fast CI:

$$\mathbf{G}_{*,i} = \mathbf{A}^H\mathbf{R}_{*,i}^{-1} = \Theta\{\mathbf{R}_{*,i}^{-1}\}. \quad (23)$$

The matrix \mathbf{G} being given column by column, the diagonal elements of matrix $\boldsymbol{\Psi}$ can be found with the following summation coming from the matrix multiplication rule:

Parameters		
Waveform		
Carrier frequency	f_0	10 GHz
Bandwidth	B	125 MHz
Range resolution	δ_R	1.2 m
PRI	T_r	1 ms
Ambiguity velocity	V_a	15 m/s
Processing parameters		
Number of ambiguities	N_a	5
Maximum velocity	V_{max}	37.5 m/s
Range oversampling	γ_t	2
Velocity oversampling	γ_v	4

Table 1. Simulated data parameters

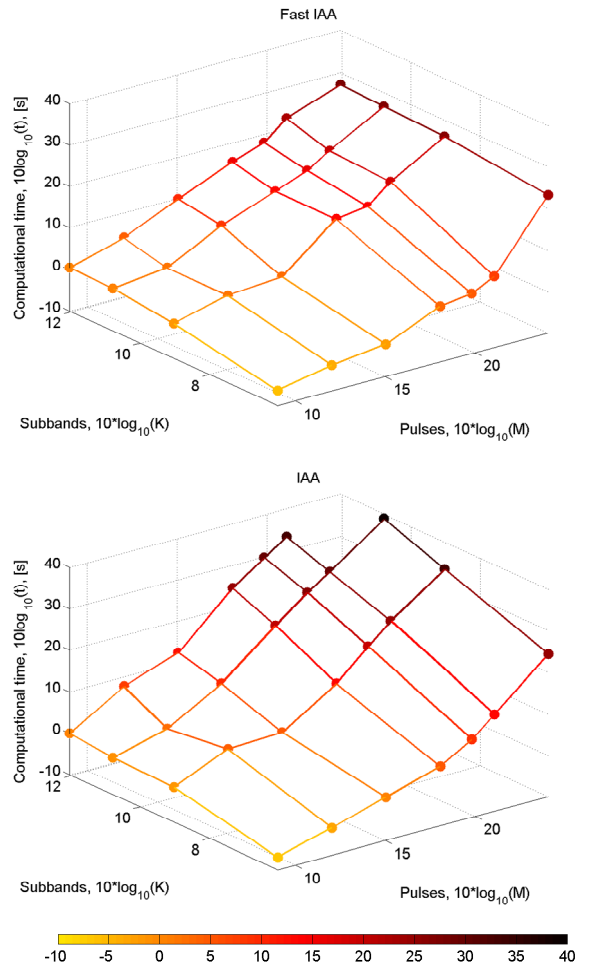


Fig. 1. Time spent on one iteration of fast IAA (top) and conventional implementation (bottom)

$$\mathbf{d} = \sum_{i=1}^{KM} \mathbf{G}_{*,i} \odot (\mathbf{A}_{i,*})^T = \sum_{i=1}^{KM} \Theta\{\mathbf{R}_{*,i}^{-1}\} \odot (\mathbf{A}_{i,*})^T, \quad (24)$$

where $()^T$ stands for matrix transpose.

Proposed way of computation is done with KM fast CI together with KM Hadamard products and thus requires $O(K^2MN_v \log_2(N_vN_t))$ operations. Note that computation complexity of this step grows similarly to the complexity of step 1 of the fast IAA.

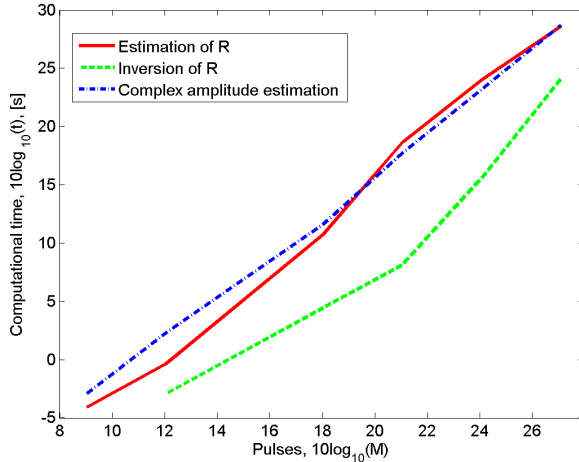


Fig. 2. Time spent on different steps of one iteration of IAA

The proposed implementation of IAA allows not to keep huge matrix \mathbf{A} in memory, and to build its rows when it is needed according to (8). This drastically decreases memory requirements of the algorithm (e.g. $K = 16$, $M = 128$, $N_a = 5$, $\gamma_t = 2$, $\gamma_v = 4$, $N_v = MN_a\gamma_v = 2560$, $N_t = \gamma_t K = 32$, then the size of \mathbf{A} is 2048×81920 , typically one complex value takes 16 bytes, thus the matrix takes 2560 MB). So the idea not to keep this matrix in memory is very attractive, especially if only a few iterations of IAA are required.

In summary, the total complexity of fast IAA is $O(KN_v \log_2(N_v N_t)) + (KM)^3/2$, while existing implementation requires $O((KM)^2 N_t N_v)$. Computational complexity of fast IAA at moderate sizes of the data are mainly limited by multiple implementation of fast CI and thus by $O(KN_v \log_2(N_v N_t))$, while for huge sizes of the problem it has cubic computational complexity of Covariance Matrix inversion $(KM)^3/2$. The gain of the fast algorithm over the existing implementation decreases when the sizes of data comes to infinity, nevertheless it is not the case in real application. The improvement for realistic data sets is studied in the next section.

6. NUMERICAL EXAMPLES

In this section the computational gain of the proposed algorithm is studied via numerical simulations in comparison to the existing implementation. This procedure is done in Matlab software on a standard PC (Intel Core i5-3470, 8 GB RAM). The synthetic data is some white noise realization, the same for the two algorithms (then matrix \mathbf{R} does not have any extra specific features). The radar parameters are mentioned in Table 1. Linear interpolation was used in Keystone transform. Time spent per one iteration of IAA is estimated and presented in Fig. 1 for both fast and conventional IAA. The number of pulses on the grid is $M = [8, 16, 32, 64, 96, 128, 256]$ and subbands is $K = [4, 8, 12, 16]$.

The presented results show more than 10 times improvement of fast IAA for moderate sizes of the problem. The dot missed in IAA plot is due to out of memory error

appearing at the step of building matrix \mathbf{A} at the corresponding sizes.

Time spent on each step of IAA is studied in the other experiment. The radar parameters are the same as in the previous simulation. LRR segment contain 16 range cells ($K = 16$) and the number of pulses (M) varies from 8 to 512 (as a power of 2). The data processed is again some realization of white noise. Fig. 2 shows the first and the third steps of the algorithm have similar complexity. The slope of time spent on Covariance Matrix inversion is higher, so at some point with high M , the matrix inversion will be the most computationally expensive operation of the algorithm (as it was shown at the previous section). Nevertheless, such huge length of data is out of interest for the presented model, since the assumption on a constant target velocity is no longer valid.

7. CONCLUSIONS

In this paper a fast implementation of Iterative Adaptive Approach with application to wideband unambiguous target detection was proposed. Specific wideband data model is shown to be a special case of non-uniform sampling of bi-dimensional complex sinusoid, thus existing fast implementations of IAA cannot be applied to this problem. The proposed algorithm allows decreasing the computational complexity by an order of magnitude for realistic data sizes, which are of practical application.

REFERENCES

- [1] F. Le Chevalier, *Principles of Radar and Sonar Signal Processing* Norwood: MA: Artech House, 2002.
- [2] R. P. Perry, R. C. DiPietro, and R. Fante, "SAR imaging of moving targets," *IEEE Transactions on Aerospace and Electronic Systems*, vol. 35, pp. 188-200, 1999.
- [3] S. Bidon, J. Y. Tourneret, L. Savy, and F. Le Chevalier, "Bayesian sparse estimation of migrating targets for wideband radar," *IEEE Transactions on Aerospace and Electronic Systems*, vol. 50, pp. 871-886, 2014.
- [4] T. Yardibi, L. Jian, P. Stoica, X. Ming, and A. B. Bagherer, "Source Localization and Sensing: A Nonparametric Iterative Adaptive Approach Based on Weighted Least Squares," *IEEE Transactions on Aerospace and Electronic Systems*, vol. 46, pp. 425-443, 2010.
- [5] X. Ming, X. Luzhou, and L. Jian, "IAA Spectral Estimation: Fast Implementation Using the Gohberg-Semencul Factorization," *IEEE Transactions on Signal Processing*, vol. 59, pp. 3251-3261, 2011.
- [6] G. O. Glentis and A. Jakobsson, "Superfast Approximative Implementation of the IAA Spectral Estimate," *IEEE Transactions on Signal Processing*, vol. 60, pp. 472-478, 2012.
- [7] S. Bidon, L. Savy, and F. Deudon, "Fast coherent integration for migrating targets with velocity ambiguity," in 2011 IEEE Radar Conference (RADAR), 2011, pp. 027-032.
- [8] A. Krishnamoorthy and D. Menon, "Matrix inversion using Cholesky decomposition," in *Signal Processing: Algorithms, Architectures, Arrangements, and Applications (SPA)*, 2013, 2013, pp. 70-72.